The Astrophysical Journal, 627:L109–L112, 2005 July 10

THE DOUBLE-PEAK SPECTRAL ENERGY DENSITY OF GAMMA-RAY BURSTS AND THE TRUE IDENTITY OF GRB 031203

Shlomo Dado[1] and Arnon Dar[1]
Received 2004 November 8; accepted 2005 May 31; published 2005 June 16

ABSTRACT

A double-peak spectral energy density of prompt γ-rays, similar to that observed in blazars, is expected in the cannonball (CB) model of gamma-ray bursts (GRBs) produced in supernova (SN) explosions. The first sub-MeV ordinary peak is formed by inverse Compton scattering (ICS) of the ambient SN light by the CBs' electrons, while the second peak at GeV-TeV energies is formed by ICS of interstellar medium electrons accelerated by the jetted CBs from the SN explosion. Usually the second peak is in the GeV-TeV range. However, in X-ray flashes with a low peak energy, which in the CB model are normal GRBs viewed far off-axis, the second peak energy moves to the MeV range. In far off-axis GRBs, such as 980425 and 031203, the second peak may have been confused with the normal GRB peak. In most GRBs that have been observed so far, the γ-ray detectors ran out of statistics far below the second peak. However, in bright GRBs, the two peaks may be resolved by simultaneous measurements with *Swift*, *INTEGRAL*, and *GLAST*.

Subject headings: gamma rays: bursts — supernovae: general

1. INTRODUCTION

There is mounting evidence that long-duration gamma-ray bursts (GRBs) and X-ray flashes (XRFs) are both produced by highly relativistic and narrowly collimated jets ejected in supernova (SN) explosions akin to SN 1998bw (e.g., Dar 2004 and references therein). Nearby XRFs seem to be ordinary GRBs whose γ-rays are much softer, and their luminosity is much lower because they are viewed from angles relative to the jet that are a few times larger than the viewing angles of ordinary GRBs (e.g., Dar & De Rújula 2000, 2004; Dado et al. 2002, 2004 and references therein). However, recently the *International Gamma-Ray Astrophysics Laboratory* (*INTEGRAL*) discovered GRB 031203 (Götz et al. 2003) at a redshift $z = 0.1055$ (Prochaska et al. 2004), the second nearest GRB after GRB 980425 at $z = 0.0085$ (Galama et al. 1998), which like GRB 980425 had extremely low luminosity, but contrary to the expectation, its γ-rays were not much softer than those of ordinary GRBs (Sazonov et al. 2004). GRB 031203 was produced in an SN very similar to SN 1998bw, which produced GRB 980425 (e.g., Malesani et al. 2004 and references therein). Consequently, the *INTEGRAL* observations were interpreted as evidence of a different class of GRBs that are produced in SNe akin to SN 1998bw, are intrinsically very faint, and include GRBs 980425 and 031203 (Sazonov et al. 2004; Soderberg et al. 2004; Woosley 2004).

The spectrum of the soft γ-rays emitted in GRB 031203, which was measured with *INTEGRAL*, is well described by $dn_\gamma/dE \sim E^{-1.63\pm0.06}$ between 20 and 400 keV (Sazonov et al. 2004). But its soft X-ray fluence in the 0.2–7 keV range, which was inferred (Watson et al. 2004) from its X-ray dust-scattered echo measured by *XMM-Newton* (Vaughan et al. 2004), is far above the *INTEGRAL* spectrum extrapolated to the soft X-ray region. It has been suggested that the soft X-ray fluence may have been overestimated (Prochaska et al. 2004; Sazonov et al. 2004).

However, in this Letter we suggest an alternative interpretation of the *INTEGRAL* and *XMM-Newton* observations, which is based on the cannonball (CB) model of GRBs and XRFs (Dar & De Rújula 2004; Dado et al. 2004) and which removes the conflicts between the off-axis interpretation of the unusually low luminosity of GRB 031203 and its high peak energy and between its soft X-ray fluence extrapolated from the *INTEGRAL* measurements (Sazonov et al. 2004) and that inferred from the *XMM-Newton* measurements (Vaughan et al. 2004). We also demonstrate that this interpretation can explain other puzzling GRB observations.

The CB model assumes that long-duration GRBs are produced by highly relativistic jets of plasmoids (CBs) of ordinary matter ejected in core-collapse SNe. Presumably, after the collapse of the stellar core into a neutron star or a black hole, an accretion disk or a torus is produced around the newly formed compact object by falling-back stellar matter (de Rújula 1987). The highly relativistic plasmoids (CBs) are emitted along the rotation axis when part of the accretion disk falls abruptly onto the compact object, as observed in microquasars (e.g., Mirabel & Rodríguez 1999; Rodríguez & Mirabel 1999 and references therein). A CB contains a thermal plasma with a power-law tail of knocked-on electrons from collisions with particles of the interstellar medium (ISM) and swept-in ISM electrons, which are Fermi-accelerated and cool quickly by synchrotron emission from the strong equipartition magnetic field in the CB. As the jet of CBs coasts through the "ambient light" permeating the surroundings of the parent SN, the electrons in the CBs Compton upscatter photons to energies that, close to the CB's direction of motion, correspond to the γ-rays of an ordinary GRB and less close to it, to the X-rays of an XRF (Dar & De Rújula 2004).

A CB also produces a narrow conical jet of high-energy cosmic-ray electrons (and nuclei) along its motion (e.g., Dar & De Rújula 2004). These electrons are of two origins: ISM electrons that were scattered elastically by the CB and ISM electrons that were Fermi-accelerated in the CB and escaped out into the ISM. These cosmic-ray electrons produce a second peak in the spectral energy density (SED) of GRBs and XRFs at a much higher energy, by inverse Compton scattering (ICS) of "ambient light" permeating the surroundings of the parent SN, like that observed in blazars (e.g., Padovani & Giommi 1995; Wehrle et al. 1998). Normal GRBs have their first peak energy usually around a fraction of an MeV and a second peak

[1] Department of Physics and Space Research Institute, Technion, Haifa 32000, Israel; dado@phep3.technion.ac.il, arnon@physics.technion.ac.il, dar@cern.ch.

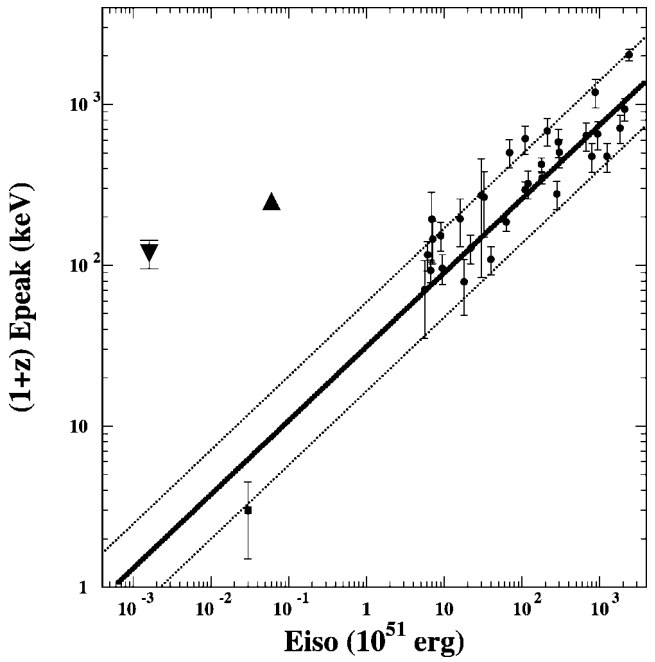

FIG. 1.—Observed rest-frame peak energy as function of the inferred isotropic radiation energy for GRBs/XRFs of known redshift and well-measured peak energy. The thick line is the best-fitted power-law correlation, $E_p \sim (E_\gamma^{\rm iso})^{0.46\pm0.04}$. The dotted lines border the estimated spread (a factor of ~4) in the isotropic radiation energy due to the spread in γ and the angular dependence of the Thomson cross section. The large outlying triangles, which represent E_p in GRB 980425 as inferred by Ghirlanda et al. (2004) and a lower limit on E_p in GRB 031203 reported by Sazonov et al. (2004), may correspond to a second peak.

energy at a much higher energy. Gamma-ray detectors on board satellites usually ran out of sensitivity/statistics well below the second peak energy. However, high-energy photons with a flux much larger than that expected from the extrapolated decline of the first peak have been discovered in a few cases of very bright GRBs with instruments on board the *Compton Gamma Ray Observatory* (*CGRO*; e.g., Hurley et al. 1994; Dingus et al. 1995; Gonzalez et al. 2003). In this Letter we demonstrate that such a high-energy component is well described by the CB model. Moreover, in very low luminosity nearby XRFs, which are far off-axis GRBs, the first peak falls in the keV range while the second peak falls in the MeV range; i.e., both peaks, or a significant fraction of both, may fall within the joint detection range of *High Energy Transient Explorer* (*HETE*), *Swift*, and *INTEGRAL*.

2. THE FIRST PEAK

Let γ be the Lorentz factor of a CB and $\delta = 1/\gamma(1 - \beta\cos\theta)$ be its Doppler factor when viewed from an angle θ relative to its motion. In the CB model (Dar & De Rújula 2004), the observed peak energy of γ-rays produced at a redshift z by ICS of thin thermal bremsstrahlung light around an SN, $dn_\gamma/dE \sim E^{-\alpha}\exp(-E/T)$ with a typical energy $\epsilon_\gamma \sim T \sim 1$ eV and $\alpha \sim 1$, is given by

$$E_p \approx \gamma\delta T/(1+z). \tag{1}$$

Under the assumption of isotropic emission in the CB rest frame, Doppler boosting and relativistic beaming yield a γ-ray fluence F_γ of a GRB pulse, which is proportional to $\gamma\delta^3$,

$$F_\gamma \approx \delta^3[(1+z)E'_\gamma/4\pi D_L^2], \tag{2}$$

where $E'_\gamma \sim N_\gamma\gamma T$ is the total energy in the CB rest frame of the N_γ ambient photons that suffer Compton scattering in the CB. Consequently, under the assumption of isotropic emission in the observer frame, the inferred "GRB isotropic γ-ray energy" in a GRB pulse is

$$E_\gamma^{\rm iso} = 4\pi D_L^2 F_\gamma/(1+z) \approx \delta^3 E'_\gamma. \tag{3}$$

If core-collapse SNe and their environments were all identical, and if their ejected CBs were also universal in number, mass, Lorentz factor, and velocity of expansion, all differences between GRBs would depend only on the observer's position, determined by z and the angle of observation, θ. For a distribution of Lorentz factors that is narrowly peaked around $\gamma \simeq 10^3$, the θ-dependence is in practice the dependence on δ, the Doppler factor. Hence equations (1) and (3) yield the correlation (Dar & De Rújula 2000, 2004)

$$(1+z)E_p \propto (E_\gamma^{\rm iso})^{1/3}, \tag{4}$$

in good agreement with the correlation $(1+z)E_p \propto (E_\gamma^{\rm iso})^k$, with $k = 0.35 \pm 0.06$ found by Amati (2004) from an analysis of a sample of 22 GRBs, which were detected and measured with instruments on board *BeppoSAX*, *CGRO*, and *HETE-2*, and whose redshift z became available from ground-based follow-up optical observations. However, equation (4) is marginally consistent with $k = 0.40 \pm 0.05$, which was found by Ghirlanda et al. (2004) from a fit to all (40) GRBs and XRFs with known redshift before 2004 June. But GRBs are far from being standard candles, and equation (4) is only a crude approximation. For instance, for GRBs with a small viewing angle, $\theta^2\gamma^2 \ll 1$, equations (1) and (3) imply $(1+z)E_p \propto \gamma^2$ and $E_\gamma^{\rm iso} \propto \gamma^4$. Then, the spread in γ yields $k = 0.5$. In the CB model, the expected value of k for the various samples of GRBs and XRFs varies between 0.33 and 0.50 (S. Dado et al. 2005, in preparation). Indeed, the best-fitted power law for $(1+z)E_p$ as a function of $E_\gamma^{\rm iso}$ for all GRBs/XRFs of known redshift, E_p and $E_\gamma^{\rm iso}$, shown in Figure 1 by a thick line, has $k = 0.46 \pm 0.05$. The parallel thin lines in Figure 1 border the expected spread around the best fit because of the spread in the "standard candle" properties of GRBs, which was found in the CB model (Dar & De Rújula 2004). As shown in Figure 1, the correlation predicted by the CB model of GRBs/XRFs is well satisfied, except by GRBs 980425 and 031203 where E_p is much larger than expected from their $E_\gamma^{\rm iso}$.

In the CB model, the predicted GRB spectrum from ICS of ambient light with a thin thermal bremsstrahlung spectrum by the electrons inside the CB is

$$\frac{dN_\gamma(1)}{dE} \propto \left(\frac{T_{\rm eff}}{E}\right)^\alpha e^{-E/T_{\rm eff}} + b(1-e^{-E/T_{\rm eff}})\left(\frac{T_{\rm eff}}{E}\right)^\beta, \tag{5}$$

where $\alpha \approx 1$, $\beta = (p+2)/2 \approx 2.1$, $T_{\rm eff} = \gamma\delta T/(1+z)$, and b is a dimensionless constant. The values of α and β may deviate from their indicated values because the ambient radiation may deviate from a thin thermal bremsstrahlung, and the power-law index of the accelerated and knocked-on electrons after cooling may be larger than $p + 1 = 3.2$ and increase with time. Also,

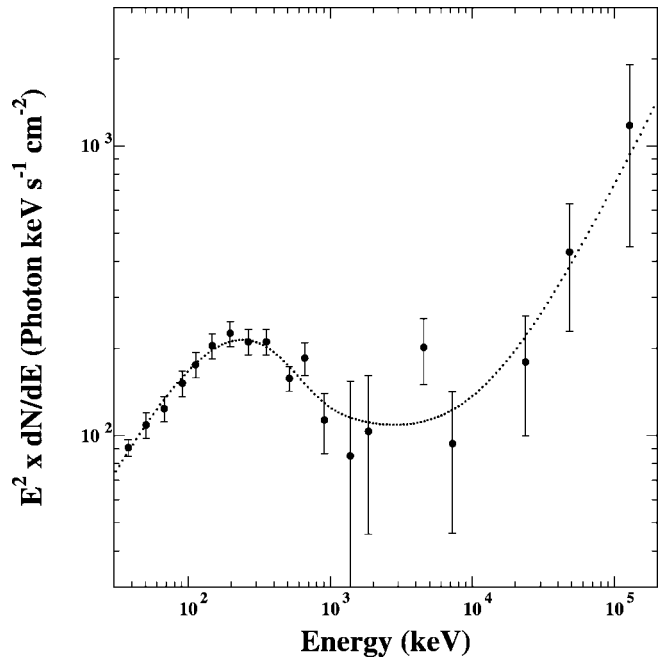

FIG. 2.—Comparison between the observed SED of GRB 941017 between 47 and 80 s after trigger (Gonzalez et al. 2003) and a CB model fit (χ^2/dof = 0.7) given by eq. (5) with $\alpha = 0.92 \pm 0.28$, $\beta = 2.23 \pm 0.14$, $T_{\rm eff} = 173 \pm 38$ keV, $b = 0.78 \pm 0.33$, and a "hard tail" proportional to E^1 as follows from eq. (8).

the ambient light temperature seen by the CB decreases with distance, as

$$T_{\rm eff}(t) \sim T_{\rm eff}(0)\{1 - \exp[-(t_0/t)^2]\}, \quad (6)$$

where t_0 is a constant. As was shown in Dar & De Rújula (2004) and in Dado et al. (2004), equation (5) is practically indistinguishable from the Band function (Band et al. 1993) and is in good agreement with the measured SED of ordinary GRBs and XRFs.

3. THE SECOND PEAK

In the CB model, the ISM in front of the CBs is ionized by the beamed radiation from the highly relativistic CBs. The turbulent magnetic fields in the CBs accelerate the ionized ISM particles, which they gather on their path, to an initial distribution, $dn_e/dE \sim E^{-p}$ with $p \sim 2.2$ in the CB rest frame. In a steady state situation, the electrons, which are trapped in the CB by its internal magnetic fields and cool quickly by synchrotron emission, reach a distribution, $dn_e/dE \sim E^{-(p+1)}$, while the electrons that escape the CB must have the hard "injection spectrum," $dn_e/dE \sim E^{-p}$. Their cooling time in the ISM is much longer than that of the electrons that are trapped magnetically inside the CBs, because the ISM magnetic field is smaller by many orders of magnitude than that inside the CBs.

In the CB rest frame, the Lorentz-boosted ambient light undergoes Compton scattering from these two distributions and produces the first peak with the "Band function" shape and a hard tail with practically a "time-independent" spectral index -1.6,

$$\frac{dN_\gamma}{dE} \propto E^{-(p+1)/2} \sim E^{-1.6}. \quad (7)$$

The ISM electrons that are scattered elastically by the highly relativistic CBs in the direction of the observer have an approximate lab energy, $E_e \sim \gamma\delta m_e$. Because of their very large Lorentz factor, $\Gamma_e \sim \gamma\delta$, the ambient photons that they scatter have much higher energies than those of the photons scattered by the "cold" electrons in the CBs, and they are narrowly beamed along the electrons' direction of motion. Hence, in the Thomson regime, they have approximately the thin thermal bremsstrahlung distribution of the ambient light boosted by $\sim 4\gamma^2\delta^2/3$:

$$E^2\frac{dN_\gamma}{dE} \propto E^{2-\alpha}e^{-E/T_{\rm eff}} \sim E^1 \quad (8)$$

for $\alpha = 1$ and $E \ll T_{\rm eff} = (4/3)\gamma^2\delta^2 T/(1+z)$. This contribution is highly beamed, and in very luminous GRBs, which are GRBs viewed near-axis, it dominates over contribution (7).

During the GRB phase, the radius of a CB increases linearly with the distance x from the explosion site while the density of the ambient light decreases like $1/x^2$. Because of the slow cooling rate in the ISM, the accumulated number of high-energy electrons in the narrow beam produced by the highly relativistic CB is proportional to the ISM mass swept up by the CB. Thus, for a constant density profile, the SED, which is proportional to the product of the swept-up mass and the density of the ambient light, increases linearly with distance, whereas it decreases like $1/x$ for a density profile of a stellar wind that blows constantly and produces a density $n_e \propto 1/x^2$. During the GRB the deceleration of the CBs is negligible and the observer time is proportional to the distance. Hence, for a constant density profile the SED increases with time like t, whereas it decreases like $1/t$ for a "windy" density profile.

In the Thomson regime, the peak energies are given approximately by $E_p \approx T_{\rm eff}/(1+z)$. Consequently, $E_p(1)$ and $E_p(2)$, the peak energies of the first and second peak, respectively, are related through

$$E_p(2) \approx (1+z)[E_p(1)]^2 T^{-1}. \quad (9)$$

For ordinary GRBs with $E_p(1) \sim 200$ keV and $z \sim 1$, equation (9) yields $E_p(2) \sim 100$ GeV, whereas for a very dim XRF with $E_p(1) \sim 1$ keV and $z \ll 1$, it yields $E_p(2) \sim 1$ MeV. Both peak energies, being proportional to $T(t)$, decrease during a GRB pulse like $T_{\rm eff}(0)\{1 - \exp[-(t_0/t)^2]\}$.

4. COMPARISON WITH OBSERVATIONS

GRB 941017.—Gonzalez et al. (2003) reported the discovery of a high-energy spectral component in GRB 940117 with an energy flux density, $E^2\,dn/dE \sim E$, peak energy $E_p(2) \geq 200$ MeV, and a fluence ≥ 3 times that of the first normal GRB component. They well fitted their data by Band functions plus a power-law contribution. The best-fitted CB model double-peak SED, which is a sum of $E^2\,dn/dE$ with dn/dE as given by equation (5) and of a second component described by equation (8) with $E \ll T_{\rm eff}(2)$, is demonstrated in Figure 2 for the SED measured between 40 and 80 s after trigger. Similar fits are obtained for the other time intervals.

GRB 031203 (Götz et al. 2003) was produced in an SN explosion similar to SN 1998bw (Malesani et al. 2004 and references therein) and had an unusually low $E_\gamma^{\rm iso}$. Its soft X-ray emission, which was inferred from modeling its measured dust-scattered echo by *XMM-Newton*, yielded a fluence in the 0.7–5 keV range (Watson et al. 2004; Vaughan et al. 2004), far above the extrapolation of the *INTEGRAL* spectrum. This

can be seen from Figure 3, in which we demonstrate a CB model fit to the SED of GRB 031203 that consists of two terms, $E^2 dn/dE$ with dn/dE as given by equation (5) for a low-energy peak with $E_p \approx T_{\rm eff} \approx 3$ keV and $b = 10^{-2}$, and a hard-tail contribution as given by equation (7). The normalization of both components was adjusted to fit the observational data. The observed photon spectral index of the hard tail, ~ -1.6, is that predicted by equation (7).

5. CONCLUSIONS

In the CB model, the CBs' internal electrons produce the sub-MeV peak in the SED of GRBs/XRFs, and the external population of high-energy (cosmic-ray) electrons, which are accelerated by the CBs, produces a second GRB peak at a much higher energy through ICS of ambient light permeating the surroundings of the parent SN. In GRBs with known redshift, the peak energy and the isotropic radiation energy of the first ordinary peak satisfy the simple correlation $(1 + z)E_p \propto (E_\gamma^{\rm iso})^{1/3-1/2}$, as predicted by the CB model. GRBs 980425 and 031203 have peak energies much larger than those expected from their very low luminosities. But in very low luminosity GRBs and XRFs that, in the CB model, are ordinary GRBs viewed far off-axis, the second peak moves down to the MeV region and can dominate the soft γ-ray region. GRBs 031203 and GRB 980425 could have been such far off-axis GRBs with their first peak in the soft X-ray region but with a second broad peak that dominates their hard X-ray and γ-ray emission, as was shown here explicitly for GRB 031203. We have also shown that the high-energy component in GRB 941017 is well explained by the second peak. Finally, we predict that simultaneous measurements with *Swift*, *INTEGRAL*, and the *Gamma-Ray Large Area Space Telescope* will resolve the spectral energy flux of ordinary GRBs/XRFs into a double-peak spectrum whose peaks move to lower energies during the GRB pulse.

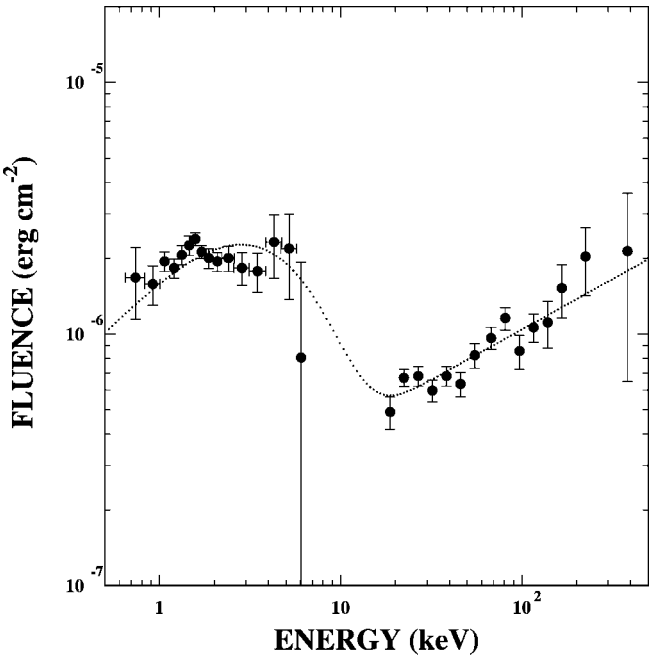

FIG. 3.—Comparison between the observed SED of GRB 031203 and a CB model fit given by eq. (5) with $E_p \approx T_{\rm eff} \approx 3$ keV and $b = 10^{-2}$, and a "hard tail" as given by eq. (7). The X-ray fluence is that inferred by Vaughan et al. (2004) from the dust echo observed with *XMM-Newton*. The *INTEGRAL* measurements are those reported by Sazonov et al. (2004).

Useful comments by Avishai Gal-Yam, Kevin Hurley, and Simon Vaughan are gratefully acknowledged. This research was supported in part by the Asher Fund for Space Research at the Technion.

REFERENCES

Amati, L. 2004, Chinese J. Astron. Astrophys., 3, 455
Band, D., et al. 1993, ApJ, 413, 281
Dado, S., Dar, A., & De Rújula, A. 2002, A&A, 388, 1079
———. 2004, A&A, 422, 381
Dar, A. 2004, preprint (astro-ph/0405386)
Dar, A., & De Rújula, A. 2000, preprint (astro-ph/0012227)
———. 2004, Phys. Rep., 405, 203
de Rújula, A. 1987, Phys. Lett. B, 193, 514
Dingus, B. L., et al. 1995, Ap&SS, 231, 187
Galama, T. J., et al. 1998, Nature, 395, 670
Ghirlanda, G., Ghisellini, G., & Lazzati, D. 2004, ApJ, 616, 331
Gonzalez, M. M., et al. 2003, Nature, 424, 749
Götz, D., Mereghetti, S., Beck, M., Borkowski, J., & Mowlavi, N. 2003, GCN Circ. 2459, http://gcn.gsfc.nasa.gov/gcn/gcn3/2459.gcn3
Hurley, K., et al. 1994, Nature, 372, 652
Malesani, D., et al. 2004, ApJ, 609, L5
Mirabel, I. F., & Rodríguez, L. F. 1999, ARA&A, 37, 409
Padovani, P., & Giommi P. 1995, ApJ, 444, 567
Prochaska, J. X., et al. 2004, ApJ, 611, 200
Rodríguez, L. F., & Mirabel, I. F. 1999, ApJ, 511, 398
Sazonov, S. U., Lutovinov, A. A., & Sunyaev, R. A. 2004, Nature, 430, 646
Soderberg, A. M., et al. 2004, Nature, 430, 648
Vaughan, S., et al. 2004, ApJ, 603, L5
Watson, D., et al. 2004, ApJ, 605, L101
Wehrle, A. E., et al. 1998, ApJ, 497, 178
Woosley, S. 2004, Nature, 430, 623